Article

Not peer-reviewed version

Investigation of the Activity of LNA-Modified Phosphorothioate Oligonucleotides Against HIV-1

Ludmila Gennadievna Gotfrid *, Kirill Artemovich Elfimov, Mariya Petrovna Gashnikova, Andrey Igorevich Murzin, Alexei Vladimirovich Totmenin, Natalia M. Gashnikova, Natalya Matveevna Gashnikova

Posted Date: 18 June 2025

doi: 10.20944/preprints202506.1545.v1

Keywords: HIV infection; modified oligonucleotides; phosphothioate modification; LNA-modification; antiretroviral activity of modified oligonucleotides; cellular internalization

 doi:10.20944/preprints202506.1545.v1

Article

Investigation of the Activity of LNA-Modified Phosphorothioate Oligonucleotides Against HIV-1

Ludmila Gotfrid *, Kirill Elfimov, Maria Gashnikova, Andrey Murzin, Aleksey Totmenin, Aleksandr Agaphonov and Natalya Gashnikova

State Research Center of Virology and Biotechnology VECTOR, Russia

* Correspondence: grushakova@inbox.ru

Abstract: This study investigated the antiretroviral efficacy, toxicity profile, and cellular uptake of LNA-modified oligonucleotides within an in vitro HIV infection model. Phosphorothioate (PS) oligonucleotides, designed to bind conserved regions of the HIV-1 genome, were modified at the 3′ and/or 5′ ends with LNA nucleotides. The antiviral properties of oligonucleotides against HIV-1 subtype A6 were evaluated using human MT-4 cell cultures. The antiretroviral activity of LNA-oligonucleotides against HIV-1 has been established. Variations in the 50% inhibitory viral reproductive dose (IC50) values among the oligonucleotides were observed, depending upon both the target and the incorporated LNA modification. The optimal IC50 values (90 ± 10 nM) were achieved using a PS oligonucleotide lacking LNA modifications, which targeted the HIV-1 integrase-encoding genomic region. Optimal IC50 values (90 ± 10 nM) were achieved using a PS oligonucleotide lacking LNA modifications, which targeted the HIV-1 integrase-encoding genomic region. Optimal HIV inhibitory action among LNA constructs was observed in an oligonucleotide with a 5′-end LNA modification targeting the HIV integrase region (IC50 = 1.12 ± 0.03 μM). The introduction of LNA modifications to PS oligonucleotides failed to enhance antiviral activity, as demonstrated by IC50 values revealing significant in vitro HIV-1 inhibitory capacity. The internalization of oligonucleotides demonstrating optimal IC50 values was investigated via flow cytometry and imaging techniques. The PS modification has been demonstrated to exhibit the highest penetration efficiency. The characteristic features included low toxicity (maintaining >92% viable cells after 48 hours of culture), high cytoplasmic membrane sorption capacity (approximately 12% FAM+ cells after 48 hours), high penetration efficiency (approximately 98% FAM+ cells showing cytoplasmic signal), and elevated internalization and entropy ratios.

Keywords: HIV infection; modified oligonucleotides; phosphothioate modification; LNA-modification; antiretroviral activity of modified oligonucleotides; cellular internalization

1. Introduction

The maximization of antiretroviral therapy (ART) treatment coverage for HIV-positive individuals has demonstrably enhanced both life expectancy and quality of life [1]. Although ART effectively reduces HIV-1 replication in humans to undetectable levels, viral latency necessitates continuous lifelong treatment [2,3]. An unavoidable consequence of this treatment is the emergence and dissemination of drug-resistant strains. For example, resistance to dolutegravir, specifically primary resistance, has been reported to range from 3.9% to 8.6%, increasing to 19.6% in individuals with a history of ART [4]. Another significant issue is the low rate of treatment adherence, especially within the youth population [5]. Resistance and low adherence, both independently and synergistically, may accelerate disease progression and restrict subsequent ART options [6]. Innovative therapeutic strategies could mitigate the adverse effects of ineffective treatment on disease progression in patients exhibiting primary resistance or poor adherence. Thus, the imperative is to research and develop drugs with new mechanisms of action against HIV.

 doi:10.20944/preprints202506.1545.v1

A potential therapeutic avenue for HIV infection involves the application of therapeutic oligonucleotides, a class of molecules with established efficacy in treating both hereditary and infectious diseases [7–12]. Antisense oligonucleotides continue to be investigated as a promising class of ARTs. Some of them have already been in the clinical trial phase. Illustrative examples include Gem92 (targeting the gag gene region), AR177 (a pol gene fragment encoding integrase), and GPs0193 (targeting the tat gene region) [13].

The mechanism of action of antisense oligonucleotides is based on blocking the translation of key viral proteins or degradation of target RNA and DNA molecules through activation of cellular nucleases such as RNase H [14], blocking the stereochemical interaction between HIV reverse transcriptase and genomic RNA [15], and inhibiting the process of reading viral mRNA matrix by the ribosome during translation [16].

The efficiency of antisense oligonucleotides is, in parallel, dependent on their ability to overcome various biological barriers, such as the cell membrane, endosomal retention, and nuclease activity (Figure 1) [17].

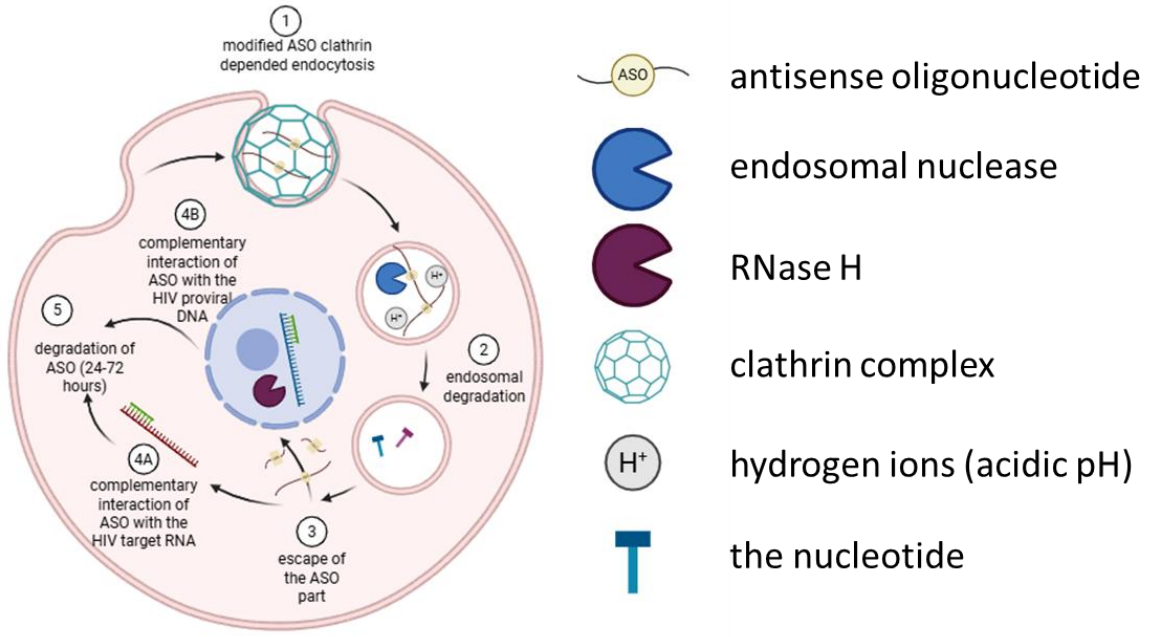

Figure 1. Membrane and intracellular transport of antisense oligonucleotides exhibiting thiophosphate and/or BNA/LNA modification.

Oligonucleotide-target interaction efficiency is enhanced through the incorporation of several chemical modifications.

Phosphorothioate (PS) modification is known to enhance oligonucleotide cellular uptake without exogenous agents or stimuli while simultaneously augmenting RNase H activity and exhibiting nuclease resistance [18,19]. Locked nucleic acid (LNA)-modifications are nucleotides in which the deoxyribose is modified by an additional bridge connecting a 2′-oxygen group to a carbon in the sugar moiety. The resulting fixed conformation leads to a higher melting point, thus enhancing resistance to denaturation and nuclease-mediated degradation [20]. LNA-modification of oligonucleotides has been reported to increase the efficiency of inhibition of virus reproduction due to increased stability of DNA duplexes and increased affinity to target sequences [16,21–25]. The nuclear and cytoplasmic accumulation of LNA-oligonucleotides mediates the degradation of HIV RNA and DNA, which incorporate complementary antisense oligonucleotide target sequences.

This study aimed to comparatively assess cellular internalization and the in vitro ability of PS/LNA-modified or just PS oligonucleotides to inhibit HIV-1 replication. The antiviral properties of oligonucleotides were examined in human lymphoid cells infected with HIV-1 subtype A6, the

 doi:10.20944/preprints202506.1545.v1

prevalent strain in the Russian HIV epidemic [26]. In addition, we evaluated the internalization efficiency of different chemical modifications of oligonucleotides in a comparative aspect.

2. Materials and Methods

Cell Culture

This work used immortalized laboratory MT-4 cell culture representing T-cell leukemia cells sourced from the NIH-ARP program. The cultivation of MT-4 cells was conducted using RPMI-1640 medium (Servicebio, China) supplemented with 10% heat-inactivated fetal bovine serum, 2 mM L-glutamine, and 20 μg/mL gentamicin in a sealed culture dish within a 37 °C, 5% CO2 incubator. The seed concentration was 350,000 cells per 1 ml of medium.

Viral Material

The HIV-1 subtype A6 strain, characterized by a rapid/high replication phenotype and significant cytopathic effect, resulted in >90% cell death by day 5. The virus was pre-inoculated on MT-4 cell culture. The infectious virus was harvested on day five of cultivation. HIV p24 concentration in viral fluids was quantified, and oligonucleotide activity was assessed using an ELISA method (HIV-1 p24-antigen-ELISA-BEST kit; Vector-Best, Russia), following the manufacturer's protocol. Reed-Muench methodology [27] was used to determine the tissue culture infectious dose (TCID50) of the virus.

Study of Antiviral Activity

Immediately before the assay, oligonucleotides were serially diluted, starting at a concentration of 10 μM and progressing in threefold increments. Three independent oligonucleotide dilution series were added to a 96-well plate previously seeded with cells. Oligonucleotides were incubated with MT-4 cells for 2 hours before HIV-1 introduction. Post-incubation, a constant dose of virus equivalent to 300 TCID50 was administered to the cell culture. The incubation with the virus was performed for 5 days in a CO_2 incubator at 37 °C and 5% CO_2. Upon completion of viral incubation with oligonucleotides, culture media samples were analyzed for p24 protein using enzyme-linked immunosorbent assay (ELISA). Three independent experimental runs yielded results that were subsequently compiled and analyzed. The values presented in the article are expressed as the mean ± standard deviation.

Imaging Flow Cytometry

The incubation of MT-4 cells with oligonucleotides was performed by adding the preparations to the nutrient medium to the final concentration. Incubation proceeded continuously throughout the experiment, with flow cytometry sampling performed at 1, 4, 12, 24, 36, and 48 hours. The culture medium contained the indicated concentration of oligonucleotides throughout the incubation period. Cellular oligonucleotide uptake was assessed using flow cytometry on the Amnis FlowSight platform (Cytek® Biosciences, USA).

A 488 nm laser with a wavelength of 60 mW was used to excite the oligonucleotide-conjugated fluorescent tag FAM, the viable PI dye, and light-field imaging (optical filters 532/55, 610/30, and 457/45, respectively). Images were acquired at a total magnification of 20× (numerical lens aperture = 0.6) and a pixel size of 1 × 1 μm. A 488 nm laser with a wavelength of 60 mW was used to excite the oligonucleotide-conjugated fluorescent tag FAM, the viable PI dye, and light-field imaging (optical filters 532/55, 610/30, and 457/45, respectively). The images were captured at 20x magnification (numerical aperture, 0.6) and a pixel resolution of 1 μm x 1 μm.

Fluorescence intensity measurements, both intra- and extra-cytoplasmic, were facilitated by the creation of cytoplasmic and membrane masks. The cytoplasmic mask was generated from a light-field image using the Adaptive Erode parameter (M01, BF, 67). The membrane mask comprised the

 doi:10.20944/preprints202506.1545.v1

parameters of the complete object mask derived from the light-field imaging channel, excluding the cytoplasm mask (Object(M01, BF, Tight) And Not AdaptiveErode(M01, BF, 67)).

Several new parameters, based on pre-existing and user-specified masks, have been introduced in the IDEAS 6.2 software. An Internalization parameter derived from the "Internalization" algorithm facilitated the determination of the internalization coefficient (IC). The second custom parameter, Entropy_1, incorporated a base Shannon entropy parameter with a granularity of 1 within the cytoplasm mask.

Statictical Analysis

The normality of data distribution was evaluated using the Shapiro-Wilk test. The homogeneity of variance was evaluated using the Levene's test. Quantitative data (most parameters) were summarized using the mean and standard deviation, while qualitative parameters (% viable cells) were described by the median and 95% confidence interval (95% CI).

The significance of variations between comparison groups was determined using ANOVA, with Fisher's criterion (F-criterion) indicated. Differences between individual oligonucleotide modifications were analyzed using a one-way analysis of variance, with subsequent pairwise comparisons employing the Tukey honestly significant difference (HSD) test to adjust for multiple comparisons. The effect size was calculated using omega-squared (ω^2), which denotes the proportion of trait variability accounted for by differences between modifications.

Within each modification, the influence of incubation time on the measured characteristics was evaluated using repeated-measures analysis of variance.

Pairwise comparisons of time points were conducted using paired t-tests, with the Benjamin-Hochberg correction applied to adjust for multiple comparisons. To determine the effect of time, a generalized eta-squared (η^2G) analysis was conducted. This metric represents the proportion of trait variance attributable to the time factor while controlling for both intra-group and inter-individual replicate variation.

Across all the comparisons, a p-value of less than 0.05 indicated statistical significance.

Statistical analysis was performed using the R programming language (v. 4.3.0, R Development Core Team, 2012; Vienna, Austria). The data were visualized using GraphPad Prism software version 10.0.0 (GraphPad Software, Boston, Massachusetts, USA).

3. Results

3.1. Oligonucleotide Design

For oligonucleotide targeting, we selected highly conserved sequences in the HIV-1 genome that are vital for the virus replication. These sequences are located in the primer-binding site region (PbS, involved in cDNA synthesis during reverse transcription), in the pol gene (Int, a gene fragment encoding a virus integrase that is responsible for integrating proviral DNA into the host cell genome), and in the HIV-1 gag gene (Gag, encoding capsid proteins; Figure 2).

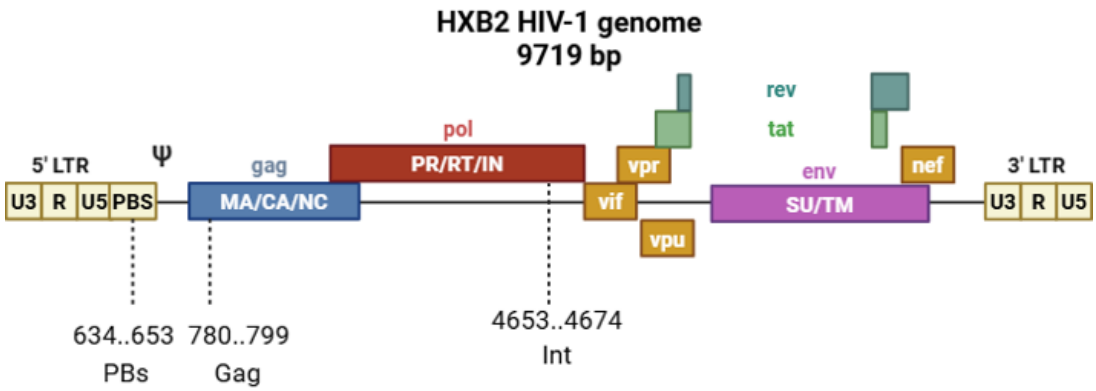

 doi:10.20944/preprints202506.1545.v1

Figure 2. Scheme of the HIV-1 HXB2 genome showing custom oligonucleotide target sites.

Our earlier work examining the internalization of oligonucleotides, modified and unmodified, showed phosphorothioate modification to be advantageous, a conclusion consistent with independent research [28–30]. Additionally, oligonucleotides containing LNA at both ends of the sequence have been previously shown to function as potent inhibitors of HIV-1 expression in cell culture [16], and this modification has been suggested to be highly promising [31].

This study evaluated the antiviral properties of phosphorothioate-modified (PS) oligonucleotides, incorporating locked nucleic acid (LNA) modifications at either or both the 3′ and 5′ ends. PS oligonucleotides similar to the target oligonucleotides without the LNA modification were used as controls. Table 1 presents a summary of the oligonucleotide derivative structures utilized in this study. Each compound underwent an evaluation of its antiretroviral activity, determining the half-maximal inhibitory concentration (IC50).

Table 1. Sequences of oligonucleotides investigated in this work.

Oligonucleotide	Sequence (5′–3′)
Oligonucleotide derivatives targeting a conserved region of the HIV-1 genome in the primer-binding site region	
PbS	$G^sT^sC^sC^sC^sT^sG^sT^sT^sC^sG^sG^sG^sC^sG^sC^sC^sA^sC^sT$
PbS_3′-LNA	$G^sT^sC^sC^sC^sT^sG^sT^sT^sC^sG^sG^sG^sC^sG^LC^LC^LA^LC^LT$
PbS_5′-LNA	$^LG^LT^LC^LC^LCT^sG^sT^sT^sC^sG^sG^sG^sC^sG^sC^sC^sA^sC^sT$
PbS_5′/3′-LNA	$^LG^LT^LC^LC^LCT^sG^sT^sT^sC^sG^sG^sG^sC^sG^LC^LC^LA^LC^LT$
Oligonucleotide derivatives targeting a conserved region encoding HIV-1 integrase	
Int	$C^sT^sT^sG^sA^sC^sT^sT^sT^sG^sG^sG^sG^sA^sT^sT^sG^sT^sA^sG^sG^sG$
Int_3′-LNA	$C^sT^sT^sG^sA^sC^sT^sT^sT^sG^sG^sG^sG^sA^sT^sT^sG^LT^LA^LG^LG^LG$
Int_5′-LNA	$^LC^LT^LT^LG^LAC^sT^sT^sT^sG^sG^sG^sG^sA^sT^sT^sG^sT^sA^sG^sG^sG$
Int_5′/3′-LNA	$^LC^LT^LT^LG^LAC^sT^sT^sT^sG^sG^sG^sG^sA^sT^sT^sG+T+A+G+G+G$
Oligonucleotide derivatives targeting a conserved region of the HIV-1 gag gene	
Gag	$T^sC^sG^sC^sA^sC^sC^sC^sA^sT^sC^sT^sC^sT^sC^sT^sC^sC^sT^sT$
Gag_3′-LNA	$T^sC^sG^sC^sA^sC^sC^sC^sA^sT^sC^sT^sC^sT^sC^LT^LC^LC^LT^LT$
Gag_5′-LNA	$^LT^LC^LG^LC^LAC^sC^sC^sA^sT^sC^sT^sC^sT^sC^sT^sC^sC^sT^sT$
Gag_5′/3′-LNA	$^LT^LC^LG^LC^LAC^sC^sC^sA^sT^sC^sT^sC^sT^sC^LT^LC^LC^LT^LT$
Oligonucleotide derivatives used for the investigation of cellular internalization capacity	
FAM-Int	[FAM]-$C^sT^sT^sG^sA^sC^sT^sT^sT^sG^sG^sG^sG^sA^sT^sT^sG^sT^sA^sG^sG^sG$
FAM-Int_3′-LNA	[FAM]-$C^sT^sT^sG^sA^sC^sT^sT^sT^sG^sG^sG^sG^sA^sT^sT^sG^LT^LA^LG^LG^LG$
FAM-Int_5′-LNA	[FAM]-$^LC^LT^LT^LG^LAC^sT^sT^sT^sG^sG^sG^sG^sA^sT^sT^sG^sT^sA^sG^sG^sG$
FAM-Int_5′/3′-LNA	[FAM]-$^LC^LT^LT^LG^LAC^sT^sT^sT^sG^sG^sG^sG^sA^sT^sT^sG+T+A+G+G+G$

Notes: S indicates the PS modification; L indicates the LNA modification; [FAM] indicates the fluorochrome tag, 6-carboxyfluorescein dye residue.

3.2. Study of Antiretroviral Activity

The antiviral efficacy of the oligonucleotides against HIV-1 strain subtype A6 was assessed using MT-4 cell suspension cultures, as detailed in the methodology section. Table 2 summarizes the specific oligonucleotide concentration at which there is a 50% suppression of HIV-1 reproduction in MT-4 cells.

 doi:10.20944/preprints202506.1545.v1

Table 2. Data on the 50% concentration (IC50) determined for oligonucleotides inhibiting HIV-1 reproduction 5 days after infection of human cells with MT-4 .

Oligonucleotide	IC_{50}, μM
PbS	0,45 ± 0,05
PbS_3′-LNA	3,27 ± 0,14
PbS_5′-LNA	3,37 ± 0,14
PbS_5′/3′-LNA	13,98 ± 0,93
Int	0,09 ± 0,01
Int_3′-LNA	1,30 ± 0,03
Int_5′-LNA	1,12 ± 0,03
Int_5′/3′-LNA	11,75 ± 0,64
Gag	0,15 ± 0,02
Gag_3′-LNA	2,34 ± 0,07
Gag_5′-LNA	2,11 ± 0,07
Gag_5′/3′-LNA	15,80 ± 0,84

The optimal IC50 values were achieved using a PS oligonucleotide targeting the HIV-1 pol gene region that encodes the viral integrase, with the IC50 determined to be 90 ± 1 nM.

The LNA-modified oligonucleotides were found to exhibit antiretroviral activity in vitro at micromolar concentrations. The discrepancies in the activity between the target oligonucleotides with identical modifications are likely attributable to variations in target accessibility within the viral genome. Our results corroborate the observations of Jakobsen et al. [16] and Takahashi et al. [29], demonstrating comparable antiviral oligonucleotide efficacy against analogous targets in conserved HIV-1 regions at micromolar concentrations (IC50).

The data analysis demonstrated that the observed differences in IC50 values were specific to oligonucleotides featuring LNA modifications. Regardless of 3′- or 5′-terminal LNA modification placement within the nucleotide sequence, antiviral activity among the tested oligonucleotides remained largely unaffected, with unmodified PS oligonucleotides demonstrating the highest HIV suppression.

An in-depth analysis of oligonucleotide cellular internalization was performed to determine the ability of the construct to enter cells.

3.3. Study of Oligonucleotide Internalization

When performing fluorescence analysis of cell populations, viable and necrotic cells were differentiated since damage to the cytoplasmic membrane in dead cells leads to nonspecific binding of fluorescent probes and may also be accompanied by an increased level of autofluorescence.

The issue mentioned above was addressed using propidium iodide, a viability marker with the property of penetrating only cells with compromised membranes to stain their DNA. Figure 3 illustrates the cell viability assessment results as a function of oligonucleotide modification.

 doi:10.20944/preprints202506.1545.v1

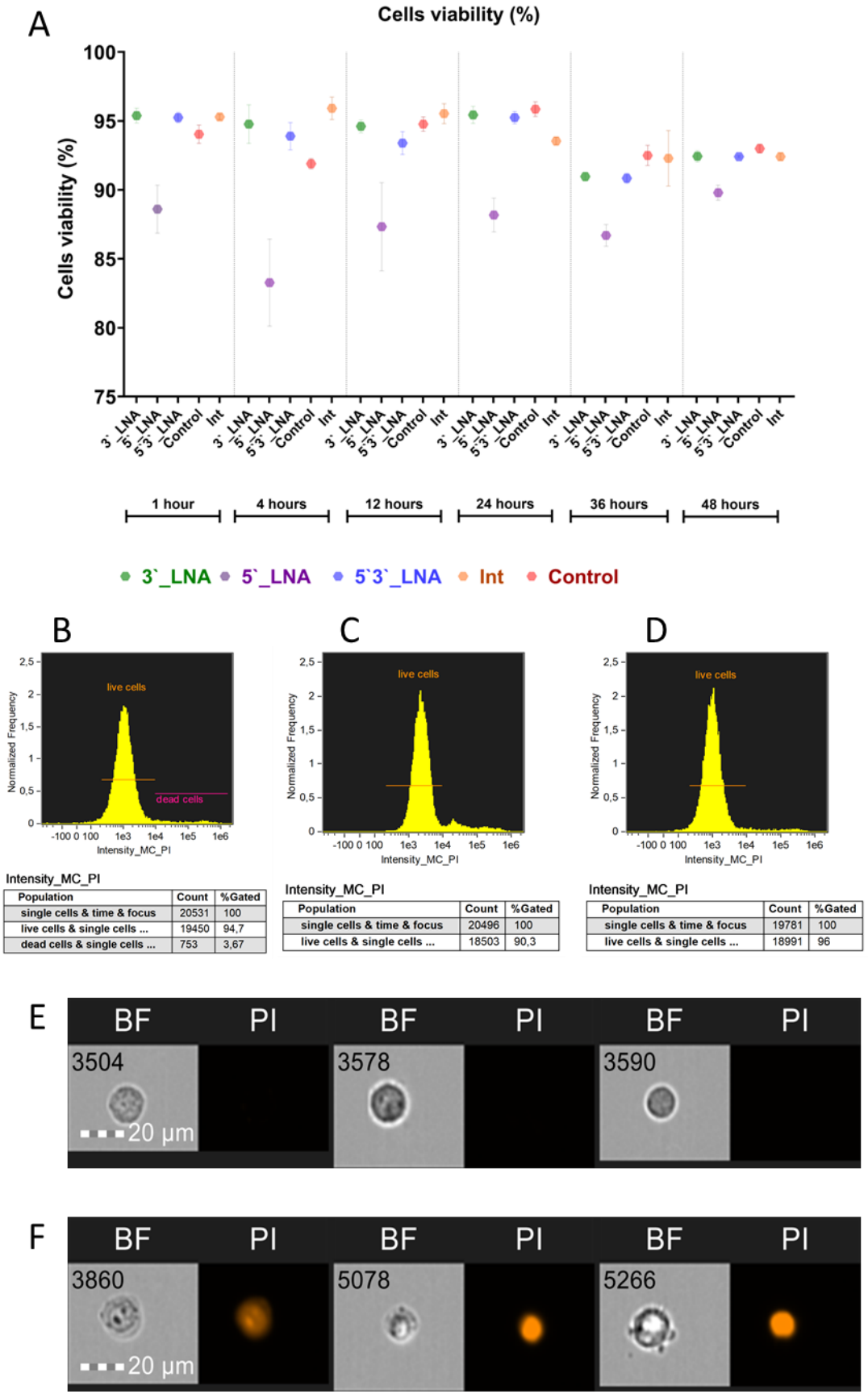

Figure 3. Cell viability of MT-4 culture cells upon the addition of oligonucleotides. (A) a graph showing cell viability as a function of added oligonucleotide modification or lack thereof (control) and time; (B) the population of live and dead cells in the control sample after one hour of culturing; (C) the population of live cells

 doi:10.20944/preprints202506.1545.v1

in the sample containing 5′-LNA oligonucleotide; (D) the population of live cells in the sample containing the 3′-LNA oligonucleotide; (E) the images of live cells with no signal in the PI channel; (F) the images of dead cells with the fluorescent signal from PI. The images used in this analysis were obtained from MT4 fixed cells using imaging flow cytometry (Cytek® Amnis® Flow Sight). The cells were stained with AOS-FAM and PI to assess cell viability. Fluorescence was excited using a 488 nm laser with a power of 60 mW. The green fluorescence from FAM was detected in the second channel using a 532/55 nm filter, while the red fluorescence from PI was detected in the third channel using a 577/35 nm filter. The images were captured at a total magnification of 20× (lens numerical aperture = 0.6), with a pixel size of 1 × 1 μm.

In most of the samples containing modified oligonucleotides, cell viability values did not show statistically significant deviations from the control group during most of the experimental period. A notable exception was the 5′-LNA modification, which significantly impaired viability. Following a 60-minute incubation period, viability was measured at 88.6 ± 1.74% (Figure 1C), subsequently declining to 83.27 ± 3.16% after 4 hours ($\eta^2 = 0.84$) and partially recovering to 89.8 ± 0.54% by 48 hours ($p = 0.338$). No statistically significant variations ($p>0.05$) were observed in the 5′-LNA-modified group, with viability decreasing steadily, unlike the control ($p<0.001$) and other modified samples ($p<0.001$ for all pairwise comparisons). The absence of full viability restoration by 48 hours could indicate a potential effect of this modification on cellular metabolism.

Cell viability following single-end 3′-LNA modification exhibited no significant difference from the control. At the one-hour mark, viability measured 95.39 ± 0.53% (Figure 3D), declining to 92.44 ± 0.41% by 48 hours. Although statistically significant temporal changes were observed ($p = 0.004$), the reduction in viability was not significantly greater than that of the control group ($p = 0.393$), suggesting a lack of specific cytotoxic effects from the 3′-LNA modification.

The penetration study determined the percentage of cells that internalized oligonucleotides, both at the membrane and within the cytoplasm (Figure 4), and the proportion of events exhibiting cytoplasmic signal from labeled nucleotides (sample internalization, see Figure 5) [32,33].

Preprints.org (www.preprints.org) | NOT PEER-REVIEWED | Posted: 18 June 2025 doi:10.20944/preprints202506.1545.v1

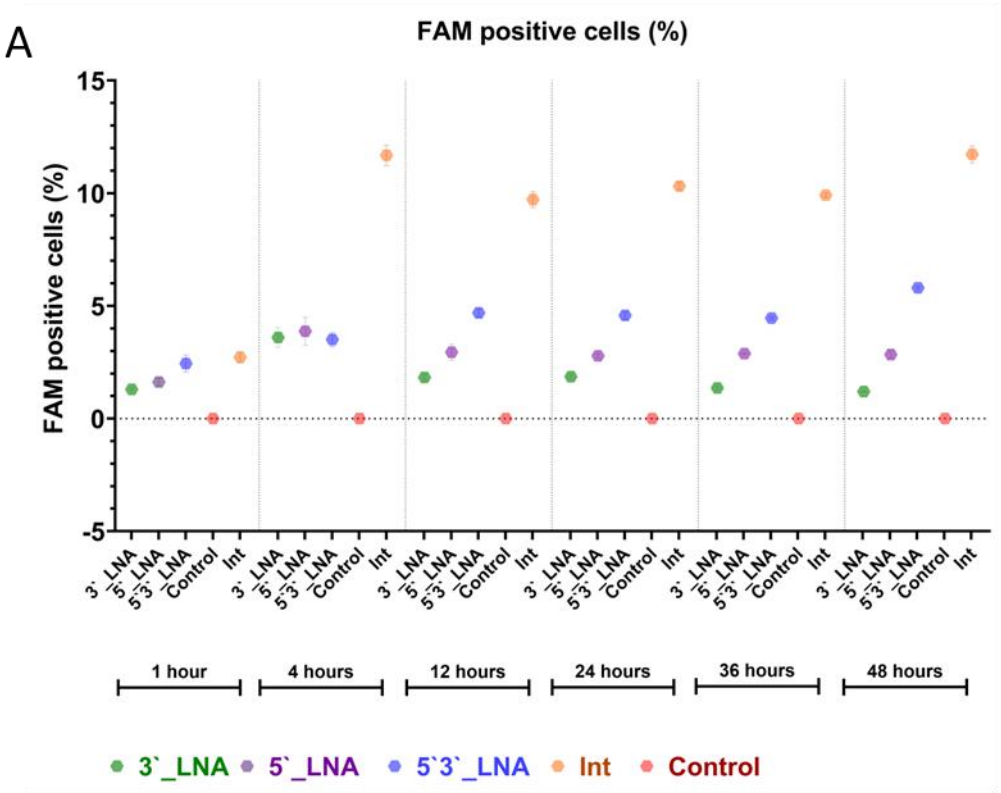

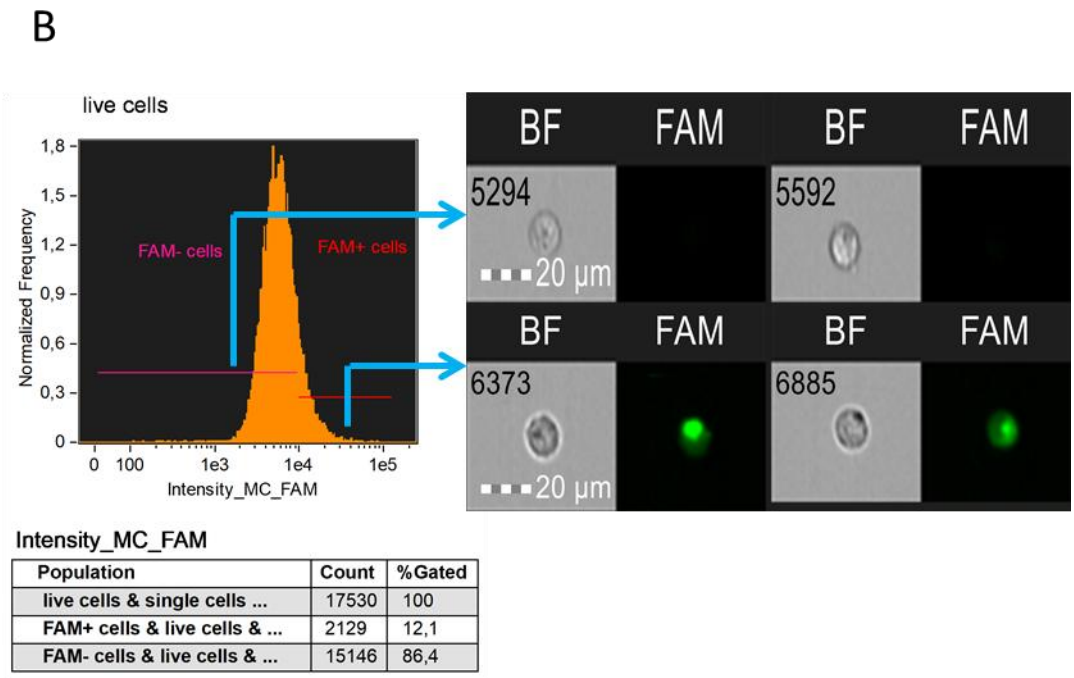

Intensity_MC_FAM

Population	Count	%Gated
live cells & single cells ...	17530	100
FAM+ cells & live cells & ...	2129	12,1
FAM- cells & live cells & ...	15146	86,4

Figure 4. Absorption of antisense oligonucleotides by MT-4 cells: (A) a graph of the dependence of the number of viable cells on the used modification and cultivation time, with the median value indicated; tendrils show the error range of the mean; (B) the demonstration of the cells from populations with and without FAM+ signal. The images used in this analysis were obtained from MT4 fixed cells using imaging flow cytometry (Cytek® Amnis® Flow Sight). The cells were stained with AOS-FAM and PI to assess cell viability. Fluorescence was excited using a 488 nm laser with a power of 60 mW. The green fluorescence from FAM was detected in the second channel using a 532/55 nm filter, while the red fluorescence from PI was detected in the third channel using a 577/35 nm filter. The images were captured at a total magnification of 20× (lens numerical aperture = 0.6), with a pixel size of 1 × 1 µm.

 doi:10.20944/preprints202506.1545.v1

The experimental data obtained demonstrate the ability of all the chemical modifications of oligonucleotides under study to interact with the cell surface. However, their efficiency was found to be significantly different depending on the place of modification introduction. The statistical analysis using the F-criterion revealed significant differences between groups ($p < 0.001$), and the effect size ($\omega^2 = 0.95 – 0.99$) confirms that the chemical structure of oligonucleotides is a key factor determining their ability for cellular uptake.

The PS-modified sample (Int) exhibited the greatest absorption efficiency. Following a 1-hour incubation period, no statistically significant difference in absorbance was observed between the unmodified oligonucleotide (Int) and the symmetrically 5′-3′ LNA-modified oligonucleotide ($p = 0.53$). However, statistically significant differences ($p < 0.001$) were detected when comparing the unmodified oligonucleotide (Int) with the terminally modified LNA variants (5′-LNA and 3′-LNA). During this period, the proportion of cells binding Int was 2.72 ± 0.243%, while the corresponding values for 5′3′-LNA, 3′-LNA, and 5′-LNA were 2.44 ± 0.374%, 1.3 ± 0.051%, and 1.62 ± 0.163%, respectively.

A four-hour incubation period revealed a statistically significant enhancement of the effects of thiophosphate modification ($p < 0.001$ for all comparisons). The observed hierarchy of uptake efficiency was Int > 5′3′LNA > 5′LNA > 3′LNA, indicating that the position of the LNA modification plays a critical role. The symmetrical arrangement (5′3′-LNA) may provide superior interaction stability within the cytoplasmic membrane and/or increased intracellular stability.

Nonetheless, the paramount metric for evaluating oligonucleotide efficacy is their capacity for cytoplasmic penetration, namely, internalization. Figure 5 presents the quantification of cytoplasm-localized, oligonucleotide-signaling cells.

 doi:10.20944/preprints202506.1545.v1

A

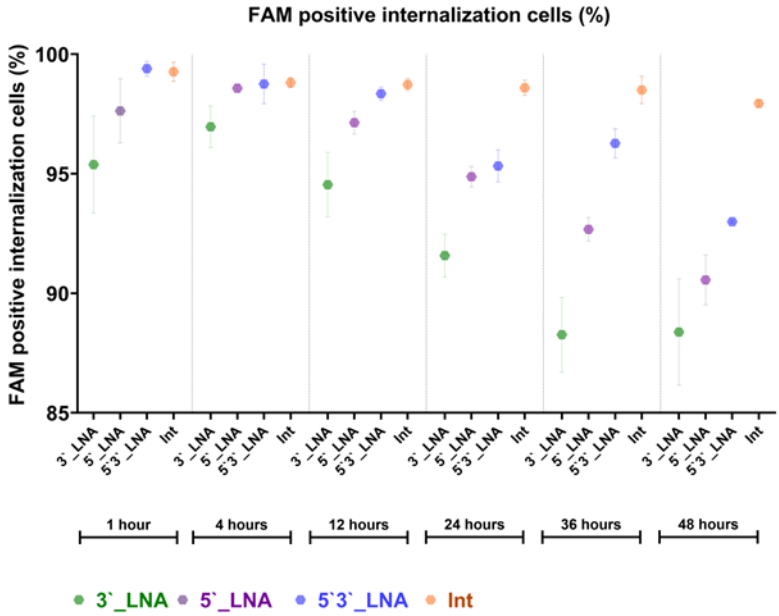

B

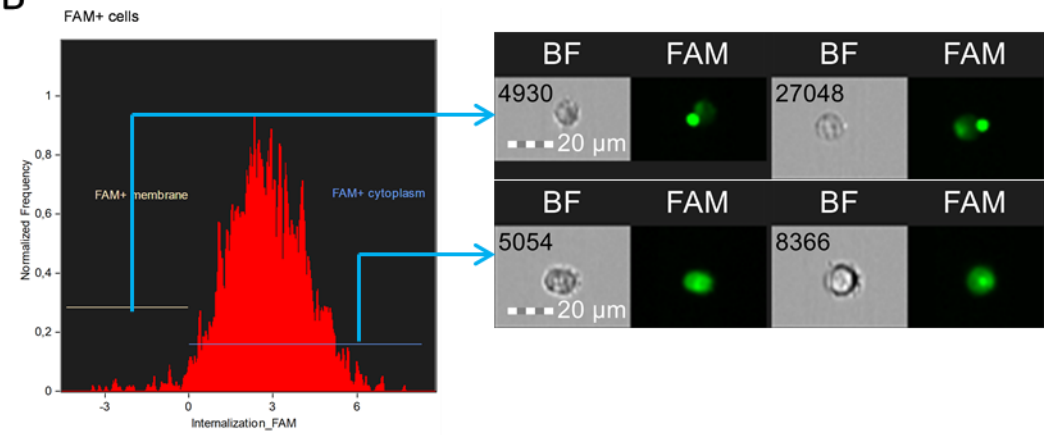

Internalization_FAM

Population	Count	%Gated	Median
FAM+ cells & live cells & ...	2129	100	2,727
FAM+ cytoplasm & FAM+ cell...	2084	97,9	2,773
FAM+ membrane & FAM+ cells...	42	1,97	-0,8748

C

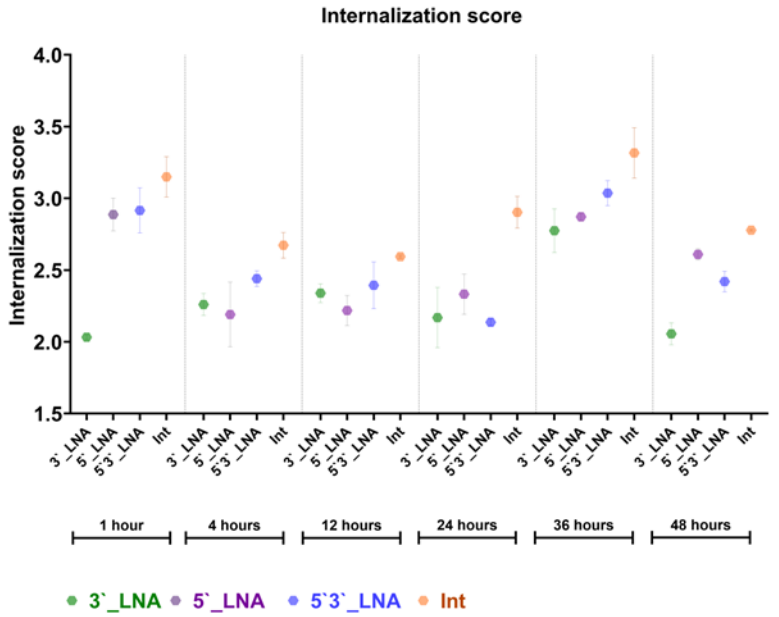

 doi:10.20944/preprints202506.1545.v1

Figure 5. Evaluation of the penetration of antisense oligonucleotides of different modifications into the cytoplasm of MT-4 cells over time: (A) the fraction of cells with intracellular FAM signal; (B) visualization of cellular populations exhibiting FAM signal both at the cell membrane and within the cytoplasm. The images used in this analysis were obtained from MT4 fixed cells using imaging flow cytometry (Cytek® Amnis® Flow Sight). The cells were stained with AOS-FAM and PI to assess cell viability. Fluorescence was excited using a 488 nm laser with a power of 60 mW. The green fluorescence from FAM was detected in the second channel using a 532/55 nm filter, while the red fluorescence from PI was detected in the third channel using a 577/35 nm filter. The images were captured at a total magnification of 20× (lens numerical aperture = 0.6), with a pixel size of 1 × 1 μm; C – the value of the internalization coefficient depends on the modification used and the time.

The data obtained demonstrate that all the tested oligonucleotide modifications, phosphothioate (Int) and LNA modification (5′3′-LNA, 5′-LNA, 3′-LNA), efficiently penetrated into the cell cytoplasm, as evidenced by the proportion of FAM+ cells exceeding 90% at the sampling time points. However, the statistical analysis revealed significant intergroup differences ($p < 0.05$), confirming the influence of chemical structure on uptake efficiency and intracellular stability.

Optimal results were observed with PS modification (Int), demonstrating FAM+ cell proportions between 92.41 ± 0.252% and 95.53 ± 0.719% throughout the incubation period (1–24 hours), with negligible variation between replicates. This observation suggests substantial resistance to degradation and stable interaction with cellular membranes.

No statistically significant difference ($p > 0.05$) in efficacy was observed between the symmetric LNA modification (5′3′-LNA) and Int within the first 12 hours of cultivation. However, by 24 hours, the difference reached statistical significance ($p < 0.05$), although the absolute difference was only 2–5%. A similar dynamics was observed for the LNA modification at the 5′-end.

The 3′-LNA modification exhibited the lowest efficiency, demonstrating a significantly reduced proportion of FAM+ cells and increased inter-replicate variability. This may result from the expedited degradation of oligonucleotides within endosomes, a process mediated by exonucleases.

Oligonucleotide penetration efficiency in MT-4 cells was assessed using two parameters: the median internalization coefficient (IC), representing the intracellular oligonucleotide fraction relative to surface-bound molecules, and entropy, reflecting uniform intracellular distribution (Figure 4C). Statistical comparisons excluded control samples exhibiting a minimal FAM+ cell population (≤0.003%).

The PS modification (Int) yielded maximal intercellular communication values at all cultivation phases. Within the initial 24-hour period, no statistically significant differences ($p > 0.05$) were observed between Int, 5′-LNA, and 5′3′-LNA, with the exception of the 12-hour mark. At this point, the IC for Int (2.59 ± 0.01) exhibited significantly higher values than that of 5′-LNA (2.22 ± 0.105; $p = 0.009$). Within 48 hours, the Int advantage had become clearly evident. The effect size ($\omega^2 = 0.6$-0.96) confirmed that it was the type of modification that caused the differences.

A comparative study of LNA variants demonstrated a correlation between internalization and the location of modification. Following up to 36 hours of cell culture, no statistically significant difference was observed between 3′ LNA and 5′ LNA or 5′/3′ LNA ($p > 0.05$). Nevertheless, a significant decrease in IC was observed by 48 hours ($p < 0.001$), while 5′3′-LNA and 5′-LNA exhibited stable ratios of 2.42 ± 0.072 and 2.61 ± 0.039, respectively.

Cellular uptake of oligonucleotides is a necessary, yet insufficient, prerequisite for functional efficacy. To bind to viral nucleic acids, oligonucleotides must evade degradation within endosomes, subsequently traversing the cytoplasm and karyoplasm to reach their primary targets (Figure 2). A key factor in their effectiveness is their ability to be uniformly distributed intracellularly, which determines their availability for interaction with target nucleic acids.

The spatial distribution of compounds was quantified using the Shannon entropy parameter, derived from FAM fluorescence intensities within a composite mask encompassing both cytoplasmic and FAM fluorescence channel regions (Figure 6). The degree of molecular dispersal is reflected by

 doi:10.20944/preprints202506.1545.v1

entropy, with higher values signifying uniform diffusion and lower values indicating aggregation or localized accumulation.

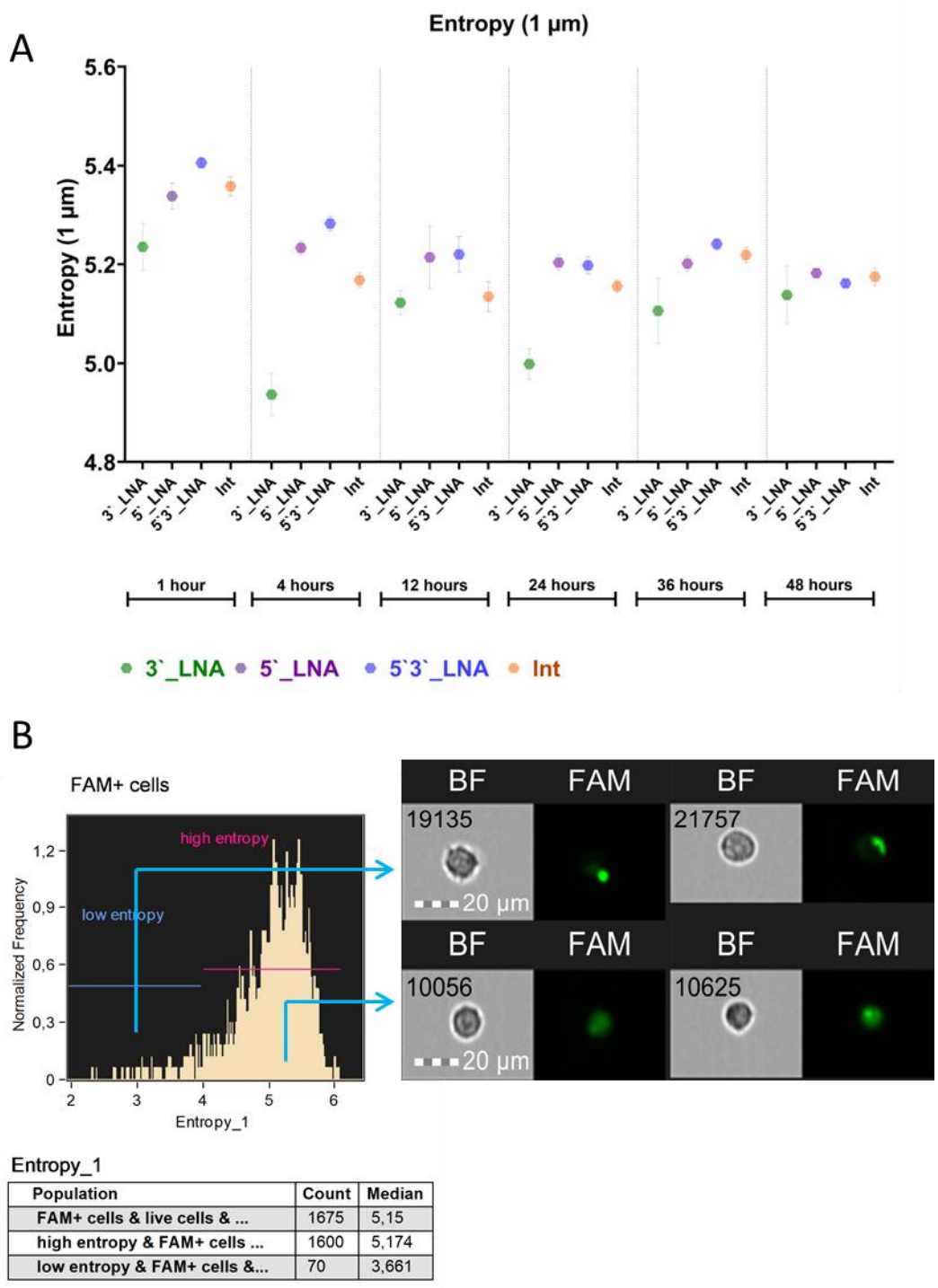

Figure 6. Results of the study of the entropy of antisense oligonucleotides in the cell cytoplasm: (A) average entropy value with average error depending on modification and cultivation time; (B) demonstration of the distribution of the FAM signal conjugated with oligonucleotides in the cytoplasm of cells with high and low entropy. The images used in this analysis were obtained from MT4 fixed cells using imaging flow cytometry (Cytek® Amnis® Flow Sight). The cells were stained with AOS-FAM and PI to assess cell viability. Fluorescence was excited using a 488 nm laser with a power of 60 mW. The green fluorescence from FAM was detected in the second channel using a 532/55 nm filter, while the red fluorescence from PI was detected in the third channel

 doi:10.20944/preprints202506.1545.v1

using a 577/35 nm filter. The images were captured at a total magnification of 20× (lens numerical aperture = 0.6), with a pixel size of 1 × 1 μm.

The findings indicate a consistent cytoplasmic distribution of all oligonucleotides within the cells, with mean values being in the range of ≥5 throughout the cultivation period. The sample modified with 5′3′-LNA displayed peak entropy within the 1- to 36-hour cultivation timeframe. Following a 48-hour culture period, thiophosphate and 5′-LNA modification levels exceeded those observed in the sample with 5′3′-LNA modification (5.18 ± 0.008 and 5.16 ± 0.006, respectively). However, these discrepancies were not statistically significant ($p = 0.948$ and $p = 0.841$).

4. Discussion

This study assessed the antiretroviral efficacy and cellular uptake of phosphorothioate oligonucleotides incorporating LNA modifications at the 3′- and/or 5′-ends of the nucleotide sequence. The rationale for these modifications was based on their established properties: enhanced resistance to nucleolytic degradation owing to the substitution of oxygen by sulfur within the phosphodiester bond [16], improved target hybridization attributable to the conformational rigidity of LNA [34], and diminished negative charge, thereby promoting interaction with the cell membrane and endocytosis [30].

The assessment of antiretroviral activity was conducted using infectious HIV-1 subtype A6 strains, with IC50 values determined. The most effective IC50 values were determined for a PS oligonucleotide directed against the integrase-coding sequence within the HIV-1 pol gene. This modification was previously studied as an inhibitor of HIV-1 gp41-mediated fusion and viral entry [35], yet a comprehensive evaluation of its cellular penetration was lacking. In an analogous study [36], the authors employed thiophosphate oligonucleotides containing imidazole and an amine group. Although several sequence variants exhibited activity, cytoplasmic uptake was not examined. The LNA modification, however, failed to improve oligonucleotide-mediated inhibition of HIV replication. The antiviral activity of oligonucleotides was most significantly reduced by incorporating LNAs at both ends of the sequence, compared to PS modification. This may reflect a reduced capacity for cellular uptake. Juliano et al. (2016) reported similar findings, attributing the reduced transmembrane permeability of excessively modified molecules to steric hindrance and compromised ligand function [30]. Alternatively, some studies indicate a greater efficacy of LNA-modified oligonucleotides when compared to unmodified antisense oligonucleotides and DNAzymes. Those studies, however, utilized a plasmid vector that included portions of the HIV genome instead of an infectious, competent isolate [16].

We investigated oligonucleotide cellular uptake via flow cytometry and imaging, quantifying absorption and penetration. Intracellular oligonucleotide distribution was characterized using the internalization coefficient (intracellular/membrane signal ratio) and entropy.

Given the characteristics investigated, the PS modification (Int) proved to be the most effective, exhibiting low toxicity (cell viability >92% at 48 h), substantial cytoplasmic membrane sorption (≈12% FAM+ cells at 48 h), significant penetration (≈98% FAM+ cells with cytoplasmic signal), and high internalization and entropy ratios.

When considering the LNA modification group, it is worth noting the advantages of single-end modification at the 5′-end and at both ends of the molecule, with similar characteristics to the PS modification in terms of internalization and entropy up to 24 hours of cultivation. However, they had fewer cells that absorbed oligonucleotides (3–6%) at the 48-hour culturing time point compared with PS (≈12%). The 3′-LNA modification exhibited enhanced toxicity and markedly reduced absorption and cellular penetration. The observed effect is likely due to the complex interaction with the cell membrane and decreased susceptibility to exonucleases initiating degradation from the 5′ end of the DNA molecule. Similar works investigating the antiretroviral activity of LNA-modified oligonucleotides have generally utilized modification at both ends of the molecule [37,38].

 doi:10.20944/preprints202506.1545.v1

5. Conclusions

A comprehensive study of phosphorothioate oligonucleotides and PS oligonucleotides with additional introduction of LNA modification at the 3′- and/or 5′-ends of the nucleotide sequence in an in vitro model of HIV infection confirmed the ability of oligonucleotides at nanomolar concentrations to inhibit HIV-1 reproduction. This study demonstrated that LNA modifications in PS oligonucleotides did not enhance antiviral activity, providing a partial explanation for the observed intracellular oligonucleotide uptake patterns across various modifications.

All the oligonucleotides under study were found to display minimal toxicity and significant cytoplasmic membrane permeability in human lymphoid cells. Furthermore, the internalization factor of the fluorescent signal from all oligonucleotides was demonstrated to exceed 2, indicating substantial intracellular penetration beyond adsorption to the cytoplasmic membrane surface. The uniform distribution of oligonucleotides within the cell cytoplasm, as described, confirms their ability to diffuse freely within cellular compartments, exhibiting marked resistance to endosomal nucleases and a uniform distribution throughout the cell's interior, improving the probability of encountering their target HIV-1 RNA.

The improved antiviral efficacy of phosphorothioate-modified oligonucleotides against HIV-1 is likely attributable to their advantageous characteristics, as demonstrated across most aspects of our investigation.

Our comparative analysis of modified oligonucleotide sets indicates that phosphorothioate oligonucleotides represent a highly promising approach to HIV-1 therapy, characterized by efficient cellular internalization and resistance to intracellular degradation.

Author Contributions: The following statements should be used: Conceptualization, N.M. Gashnikova and A.V. Totmenin; methodology, L.G. Gotfrid, K.A. Elfimov, A.I. Murzin and M.P. Gashnikova; software, K.A. Elfimov, A.I. Murzin; formal analysis, K.A. Elfimov.; investigation, L.G. Gotfrid, K.A. Elfimov and M.P. Gashnikova; data curation, N.M. Gashnikova and A.V. Totmenin.; writing—original draft preparation, L.G. Gotfrid, K.A. Elfimov, A.I. Murzin; writing—review and editing, , N.M. Gashnikova; visualization, K.A. Elfimov, A.I. Murzin; project administration, A.P. Agafonov; funding acquisition, N.M. Gashnikova, A.P. Agafonov. All authors have read and agreed to the published version of the manuscript.

Funding: State Assignment no. 1/23 (FBRI SRC VB 'Vector' Rospotrebnadzor) supported this research.

Institutional Review Board Statement: Not applicable.

Informed Consent Statement: Not applicable.

Data Availability Statement: The datasets presented in this article are not readily available because due to technical limitations. Requests to access the datasets should be directed to corresponding author.

Acknowledgments: We would like to thank Alina Nokhova for her advice on choosing statistical criteria for analyzing flow cytometry results.

Conflicts of Interest: The authors declare no conflicts of interest.

References

1. Menéndez-Arias, L.; Delgado, R. Update and Latest Advances in Antiretroviral Therapy. Trends in Pharmacological Sciences 2022, 43, 16–29, doi:10.1016/j.tips.2021.10.004.
2. Vanhamel, J.; Bruggemans, A.; Debyser, Z. Establishment of Latent HIV-1 Reservoirs: What Do We Really Know? Journal of Virus Eradication 2019, 5, 3–9, doi:10.1016/S2055-6640(20)30275-2.
3. Dufour, C.; Gantner, P.; Fromentin, R.; Chomont, N. The Multifaceted Nature of HIV Latency. Journal of Clinical Investigation 2020, 130, 3381–3390, doi:10.1172/JCI136227.
4. Bertagnolio, S.; Hermans, L.; Jordan, M.R.; Avila-Rios, S.; Iwuji, C.; Derache, A.; Delaporte, E.; Wensing, A.; Aves, T.; Borhan, A.S.M.; et al. Clinical Impact of Pretreatment Human Immunodeficiency Virus Drug Resistance in People Initiating Nonnucleoside Reverse Transcriptase Inhibitor–Containing Antiretroviral

 doi:10.20944/preprints202506.1545.v1

Therapy: A Systematic Review and Meta-Analysis. The Journal of Infectious Diseases 2021, 224, 377–388, doi:10.1093/infdis/jiaa683.

5. Zurbachew, Y.; Hiko, D.; Bacha, G.; Merga, H. Adolescent's and Youth's Adherence to Antiretroviral Therapy for Better Treatment Outcome and Its Determinants: Multi-Center Study in Public Health Facilities. AIDS Res Ther 2023, 20, 91, doi:10.1186/s12981-023-00588-y.
6. Sitanggang, H.D.; Wahyono, T.Y.M.; Ayu, I.M. Effect of Non-Adherence to ARV Therapy on 3-Year Life of HIV/AIDS Patients: A Cohort Retrospective Study. RIK 2023, 12, 1, doi:10.30644/rik.v12i1.692.
7. González, V.; Martín, M.; Fernández, G.; García-Sacristán, A. Use of Aptamers as Diagnostics Tools and Antiviral Agents for Human Viruses. Pharmaceuticals 2016, 9, 78, doi:10.3390/ph9040078.
8. Perrone, R.; Butovskaya, E.; Lago, S.; Garzino-Demo, A.; Pannecouque, C.; Palù, G.; Richter, S.N. The G-Quadruplex-Forming Aptamer AS1411 Potently Inhibits HIV-1 Attachment to the Host Cell. International Journal of Antimicrobial Agents 2016, 47, 311–316, doi:10.1016/j.ijantimicag.2016.01.016.
9. Xun, J.; Zhang, X.; Guo, S.; Lu, H.; Chen, J. Editing out HIV: Application of Gene Editing Technology to Achieve Functional Cure. Retrovirology 2021, 18, 39, doi:10.1186/s12977-021-00581-1.
10. Del Corpo, O.; Goguen, R.P.; Malard, C.M.G.; Daher, A.; Colby-Germinario, S.; Scarborough, R.J.; Gatignol, A. A U1i RNA That Enhances HIV-1 RNA Splicing with an Elongated Recognition Domain Is an Optimal Candidate for Combination HIV-1 Gene Therapy. Molecular Therapy Nucleic Acids 2019, 18, 815–830, doi:10.1016/j.omtn.2019.10.011.
11. Virgilio, A.; Esposito, V.; Tassinari, M.; Nadai, M.; Richter, S.N.; Galeone, A. Novel Monomolecular Derivatives of the Anti-HIV-1 G-Quadruplex-Forming Hotoda's Aptamer Containing Inversion of Polarity Sites. European Journal of Medicinal Chemistry 2020, 208, 112786, doi:10.1016/j.ejmech.2020.112786.
12. Ceña-Diez, R.; Singh, K.; Spetz, A.-L.; Sönnerborg, A. Novel Naturally Occurring Dipeptides and Single-Stranded Oligonucleotide Act as Entry Inhibitors and Exhibit a Strong Synergistic Anti-HIV-1 Profile. Infect Dis Ther 2022, 11, 1103–1116, doi:10.1007/s40121-022-00626-8.
13. Gheibi-Hayat, S.M.; Jamialahmadi, K. Antisense Oligonucleotide (AS-ODN) Technology: Principle, Mechanism and Challenges. Biotech and App Biochem 2021, 68, 1086–1094, doi:10.1002/bab.2028.
14. Shen, W.; De Hoyos, C.L.; Migawa, M.T.; Vickers, T.A.; Sun, H.; Low, A.; Bell, T.A.; Rahdar, M.; Mukhopadhyay, S.; Hart, C.E.; et al. Chemical Modification of PS-ASO Therapeutics Reduces Cellular Protein-Binding and Improves the Therapeutic Index. Nat Biotechnol 2019, 37, 640–650, doi:10.1038/s41587-019-0106-2.
15. Hatta, T.; Kim, S.-G.; Nakashima, H.; Yamamoto, N.; Sakamoto, K.; Yokoyama, S.; Takaku, H. Mechanisms of the Inhibition of Reverse Transcription by Unmodified and Modified Antisense Oligonucleotides. FEBS Letters 1993, 330, 161–164, doi:10.1016/0014-5793(93)80264-U.
16. Jakobsen, M.R.; Haasnoot, J.; Wengel, J.; Berkhout, B.; Kjems, J. Efficient Inhibition of HIV-1 Expression by LNA Modified Antisense Oligonucleotides and DNAzymes Targeted to Functionally Selected Binding Sites. Retrovirology 2007, 4, 29, doi:10.1186/1742-4690-4-29.
17. Shadid, M.; Badawi, M.; Abulrob, A. Antisense Oligonucleotides: Absorption, Distribution, Metabolism, and Excretion. Expert Opinion on Drug Metabolism & Toxicology 2021, 17, 1281–1292, doi:10.1080/17425255.2021.1992382.
18. Crooke, S.T.; Seth, P.P.; Vickers, T.A.; Liang, X. The Interaction of Phosphorothioate-Containing RNA Targeted Drugs with Proteins Is a Critical Determinant of the Therapeutic Effects of These Agents. J. Am. Chem. Soc. 2020, 142, 14754–14771, doi:10.1021/jacs.0c04928.
19. Crooke, S.T.; Vickers, T.A.; Liang, X. Phosphorothioate Modified Oligonucleotide–Protein Interactions. Nucleic Acids Research 2020, 48, 5235–5253, doi:10.1093/nar/gkaa299.
20. Hagedorn, P.H.; Persson, R.; Funder, E.D.; Albæk, N.; Diemer, S.L.; Hansen, D.J.; Møller, M.R.; Papargyri, N.; Christiansen, H.; Hansen, B.R.; et al. Locked Nucleic Acid: Modality, Diversity, and Drug Discovery. Drug Discovery Today 2018, 23, 101–114, doi:10.1016/j.drudis.2017.09.018.
21. Stincarelli, M.A.; Rocca, A.; Antonelli, A.; Rossolini, G.M.; Giannecchini, S. Antiviral Activity of Oligonucleotides Targeting the SARS-CoV-2 Genomic RNA Stem-Loop Sequences within the 3′-End of the ORF1b. Pathogens 2022, 11, 1286, doi:10.3390/pathogens11111286.

 doi:10.20944/preprints202506.1545.v1

22. Hagey, R.J.; Elazar, M.; Pham, E.A.; Tian, S.; Ben-Avi, L.; Bernardin-Souibgui, C.; Yee, M.F.; Moreira, F.R.; Rabinovitch, M.V.; Meganck, R.M.; et al. Programmable Antivirals Targeting Critical Conserved Viral RNA Secondary Structures from Influenza A Virus and SARS-CoV-2. Nat Med 2022, 28, 1944–1955, doi:10.1038/s41591-022-01908-x.
23. Dowerah, D.; V. N. Uppuladinne, M.; Sarma, P.J.; Biswakarma, N.; Sonavane, U.B.; Joshi, R.R.; Ray, S.K.; Namsa, N.D.; Deka, R.Ch. Design of LNA Analogues Using a Combined Density Functional Theory and Molecular Dynamics Approach for RNA Therapeutics. ACS Omega 2023, 8, 22382–22405, doi:10.1021/acsomega.2c07860.
24. Hillebrand, F.; Ostermann, P.N.; Müller, L.; Degrandi, D.; Erkelenz, S.; Widera, M.; Pfeffer, K.; Schaal, H. Gymnotic Delivery of LNA Mixmers Targeting Viral SREs Induces HIV-1 mRNA Degradation. IJMS 2019, 20, 1088, doi:10.3390/ijms20051088.
25. Riera-Tur, I.; Hinterdobler, J.; Maaske, A.; Sadewasser, A.; Schell, M.; Sekar, J.; Michel, S.; Klar, R.; Jaschinski, F. Characterization of the TLR9-Activating Potential of LNA-Modified Antisense Oligonucleotides. Nucleic Acid Therapeutics 2024, 34, 257–271, doi:10.1089/nat.2024.0013.
26. Kirichenko, A.; Lapovok, I.; Baryshev, P.; Van De Vijver, D.A.M.C.; Van Kampen, J.J.A.; Boucher, C.A.B.; Paraskevis, D.; Kireev, D. Genetic Features of HIV-1 Integrase Sub-Subtype A6 Predominant in Russia and Predicted Susceptibility to INSTIs. Viruses 2020, 12, 838, doi:10.3390/v12080838.
27. Reed, L.J.; Muench, H. A SIMPLE METHOD OF ESTIMATING FIFTY PER CENT ENDPOINTS12. American Journal of Epidemiology 1938, 27, 493–497, doi:10.1093/oxfordjournals.aje.a118408.
28. Crooke, S.T.; Wang, S.; Vickers, T.A.; Shen, W.; Liang, X. Cellular Uptake and Trafficking of Antisense Oligonucleotides. Nat Biotechnol 2017, 35, 230–237, doi:10.1038/nbt.3779.
29. Takahashi, M.; Li, H.; Zhou, J.; Chomchan, P.; Aishwarya, V.; Damha, M.J.; Rossi, J.J. Dual Mechanisms of Action of Self-Delivering, Anti-HIV-1 FANA Oligonucleotides as a Potential New Approach to HIV Therapy. Molecular Therapy - Nucleic Acids 2019, 17, 615–625, doi:10.1016/j.omtn.2019.07.001.
30. Juliano, R.L. The Delivery of Therapeutic Oligonucleotides. Nucleic Acids Res 2016, 44, 6518–6548, doi:10.1093/nar/gkw236.
31. Zhou, J.; Satheesan, S.; Li, H.; Weinberg, M.S.; Morris, K.V.; Burnett, J.C.; Rossi, J.J. Cell-Specific RNA Aptamer against Human CCR5 Specifically Targets HIV-1 Susceptible Cells and Inhibits HIV-1 Infectivity. Chemistry & Biology 2015, 22, 379–390, doi:10.1016/j.chembiol.2015.01.005.
32. Vranic, S.; Boggetto, N.; Contremoulins, V.; Mornet, S.; Reinhardt, N.; Marano, F.; Baeza-Squiban, A.; Boland, S. Deciphering the Mechanisms of Cellular Uptake of Engineered Nanoparticles by Accurate Evaluation of Internalization Using Imaging Flow Cytometry. Part Fibre Toxicol 2013, 10, 2, doi:10.1186/1743-8977-10-2.
33. Phanse, Y.; Ramer-Tait, A.E.; Friend, S.L.; Carrillo-Conde, B.; Lueth, P.; Oster, C.J.; Phillips, G.J.; Narasimhan, B.; Wannemuehler, M.J.; Bellaire, B.H. Analyzing Cellular Internalization of Nanoparticles and Bacteria by Multi-Spectral Imaging Flow Cytometry. JoVE 2012, 3884, doi:10.3791/3884.
34. Koshkin, A.A.; Nielsen, P.; Meldgaard, M.; Rajwanshi, V.K.; Singh, S.K.; Wengel, J. LNA (Locked Nucleic Acid): An RNA Mimic Forming Exceedingly Stable LNA:LNA Duplexes. J. Am. Chem. Soc. 1998, 120, 13252–13253, doi:10.1021/ja9822862.
35. Vaillant, A.; Juteau, J.-M.; Lu, H.; Liu, S.; Lackman-Smith, C.; Ptak, R.; Jiang, S. Phosphorothioate Oligonucleotides Inhibit Human Immunodeficiency Virus Type 1 Fusion by Blocking Gp41 Core Formation. Antimicrob Agents Chemother 2006, 50, 1393–1401, doi:10.1128/AAC.50.4.1393-1401.2006.
36. Ushijima, K.; Shirakawa, M.; Kagoshima, K.; Park, W.-S.; Miyano-Kurosaki, N.; Takaku, H. Anti-HIV-1 Activity of an Antisense Phosphorothioate Oligonucleotide Bearing Imidazole and Primary Amine Groups. Bioorganic & Medicinal Chemistry 2001, 9, 2165–2169, doi:10.1016/S0968-0896(01)00126-2.
37. Ivanova, G.; Arzumanov, A.; Gait, M.J.; Reigadas, S.; Toulmé, J.-J.; Andreola, M.-L.; Ittig, D.; Leumann, C. Comparative Studies of Tricyclo-DNA- and LNA-Containing Oligonucleotides as Inhibitors of HIV-1 Gene Expression. Nucleosides, Nucleotides and Nucleic Acids 2007, 26, 747–750, doi:10.1080/15257770701490928.
38. Pedersen, E.B.; Nielsen, J.T.; Nielsen, C.; Filichev, V.V. Enhanced Anti-HIV-1 Activity of G-Quadruplexes Comprising Locked Nucleic Acids and Intercalating Nucleic Acids. Nucleic Acids Research 2011, 39, 2470–2481, doi:10.1093/nar/gkq1133.

 doi:10.20944/preprints202506.1545.v1